International Journal of Technology 11(2) 248-258 (2020)
Received September 2019 / Revised October 2019 / Accepted February 2020

International Journal of Technology

http://ijtech.eng.ui.ac.id

# Rheology Characteristics and Critical Velocity of Particle-laden Flow Affected by Three-lobed Spiral Pipe

Sealtial Mau[1], Yanuar [1*], Agus S. Pamitran [1]

[1]*Department of Mechanical Engineering, Faculty of Engineering, Universitas Indonesia, Kampus UI Depok, Depok 16424, Indonesia*

**Abstract**. The use of piping systems for fluid transportation is increasing because it is considered the most effective method. Newtonian and non-Newtonian fluid flows are suitable for piping systems, and non-Newtonian, particle-laden fluids are more complex due to various factors. Deposition is one of the problems that must continue to be investigated because of the effects of flow efficiency. The purpose of this study was to investigate the performance of the three-lobe spiral pipe effect. Working fluids in several variations of concentration weight (Cw 20%, 30%, and 40%) were used. Test pipe with a length of 1550 mm and consisting of spiral pipe P/Di = 7 and a circular pipe with an inner diameter of 25.4 mm were used. The circular pipe was used to investigate the rheological workings of fluid. Both pipes were used to investigate the particle effects. Using scanning electron microscopy, 1-μm to 5-μm slurry particles were obtained from the mud eruption source at Semau Island, Kupang, Indonesia. The critical velocity value of the spiral pipe was lower than the circular pipe, so the spiral pipe is highly effective for slurry transportation.

*Keywords:* non-Newtonian; Particle solid; Passive control; Pressure drop; Spiral pipe

## 1. Introduction

The piping system is considered the most effective medium of liquid transportation and is widely used in industrial and engineering productivity (Steffe, 1992; Priadi et al., 2017; Deka et al., 2018). Newtonian and non-Newtonian fluid flows are appropriate for transportation by piping systems. Although both fluids can flow in a pipe, non-Newtonian flow is more complex. Various studies have been carried out to produce efficient flow while reducing energy consumption. Two methods developed to obtain drag reduction are the active and passive control methods. The active control method is adds substances or additives to be better affect the flow through the working fluid (Gad-el-Hak et al., 2003). The passive control method is used to form the channel geometry needed to obtain a more effective fluid flow structure for the working fluid (Ganeshalingam, 2002).

Various pipe cross-sections have been used as solutions for problems in piping systems, such as rectangular pipes, pentagon spiral pipes, and spiral pipes with three- and four-lobed variations (Watanabe et al., 1984; Watanabe and Yanuar, 1996; Ariyaratne, 2005; Selvaraj et al., 2011; Mau and Yanuar, 2018). The appropriate pipe geometry for working fluid is reasonable to facilitate the flow efficiency. Siswantara et al. conducted a simulation study on the first step to predicting the slurry flow in an anaerobic digester

*Corresponding author's email: yanuar@eng.ui.ac.id, Tel.: +62-818897518, Fax. +62-217270033
doi: 10.14716/ijtech.v11i2.3506

(Siswantara et al., 2016). The study was conducted with a numerical simulation method to achieve the correct planning basis so that the development of the digester was carried out efficiently. Matousek argued that each piping system designed for slurry must consider flow performance (Matousek, 2005). He assumed that it was more important to understand the permanent contact between the particles and the wall than the sporadic contact (collision) between particles. Matoušek's assertion about the contact of slurry particles with the wall will be deeply analyzed in future research. Maruyama et al. conducted an investigation to study the solid effect in two-phase flow (Maruyama et al, 1979). He stated that deposits of solid particles can be reduced by the vortex flow, which is called vertical motion.

On the other hand, both influences of pipe wall geometry and surfactant revealed by Yanuar combined the active and passive control methods (Yanuar et al., 2012; Yanuar et al., 2015). In their study, drag reduction was not influenced only by a mixture of drag-reducing agents but also by the wall of pipe geometry.

Several previous studies related to piping systems have been carried out in conjunction with the impact on environmental losses and energy efficiency (Senapati et al., 2013; Yanuar et al., 2018). The particle-laden fluid flow transport characteristics of solid water mixtures in piping systems need to be thoroughly understood so that it can be used to solve piping application problems. Kim et al. revealed that when the mean velocity is higher than the critical velocity, hydraulic gradient of working fluid flowing through square duct is larger than that through circular pipe (Kim et al., 2008). This research carried out as an approach solution in piping system calculation for mud eruption in Indonesia that is detrimental the citizens, causing the loss of their homes and fields (Marbun, 2015; The Jakarta Post, 2015). The solid particles for the working fluid mixtures were obtained from a mud eruption in Semau Island, Kupang, Indonesia. For the apparatus setup, a spiral pipe with a three-lobed cross-section was used as it has been proved to be more efficient for two-phase flow with high viscosity. The purpose of this study was to investigate the performance of three-lobed spiral pipe for the transportation of working fluids with 20%, 30%, and 40% concentration weights, Cw. The aim of the investigation was to reveal the impact of friction and particles by using three-lobed spiral pipe.

## 2. Methods

Both horizontal pipes of circular and three-lobed spiral were used as the main test pipe in this experiment, as shown schematically in Figure 1. Circular pipe with a 25.4-mm inner diameter and spiral pipe with an inner diameter of $D_i$, an outer diameter of $D_o$, and a difference between the inner diameter and outer diameter of $\Delta D$ were used, as in the table 1. The length of the pipe cross-section rotated as much as $360^o$, which is defined as the pitch. The $P/D_i$ is defined as the ratio of the pitch to the inner diameter. The P/Di variation of spiral pipe was used to determine the drag reduction impact and the highest drag reduction was obtained on the spiral pipe with P/Di= 7 (Yanuar et al., 2015). Figure 2 shows the schematic of the experimental setup of this study. A slurry agitator of 1500 rpm was operated during the test to prevent agglomeration. The working fluid was flowed to the test pipe using a slurry pump and was gradually flowed using a regulator valve. Before reaching the main test pipe, the working fluid crossed the pipe section that was set to obtain full development flow with a length of 40D.

The pressure taps in the main pipe were equipped with different pressure measurement sensors to collect data on the pressure drop. The sensor used (EMANT300) was a compact 24-bit data acquisition (DAQ) module developed for learning purposes. The sensor can be calibrated to obtain measurement results with minimal errors that are exceptionally relevant for laboratory-scale research. In this experiment, the room

temperature was kept constant at 25°C. The entrance flow variations were regulated using the valve regulator from the minimum to the maximum. Every valve variation which is setup at each time interval and the test fluid that flowed was collected on a container and then weighed using a digital scale with a high level of accuracy.

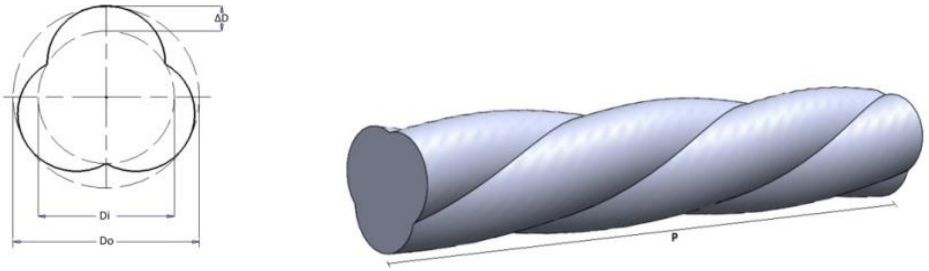


(a) Front view (b) Side view

**Figure 1**. Spiral pipe geometry

**Table 1** Test pipe dimensions

| Pipes | Di (mm) | Do (mm) | ΔD (mm) | P (Pitch) | P/Di |
|---|---|---|---|---|---|
| Circular | 25.4 | 25.4 | - | - | - |
| Spiral | 37 | 47.6 | 5.3 | 259 | 7 |

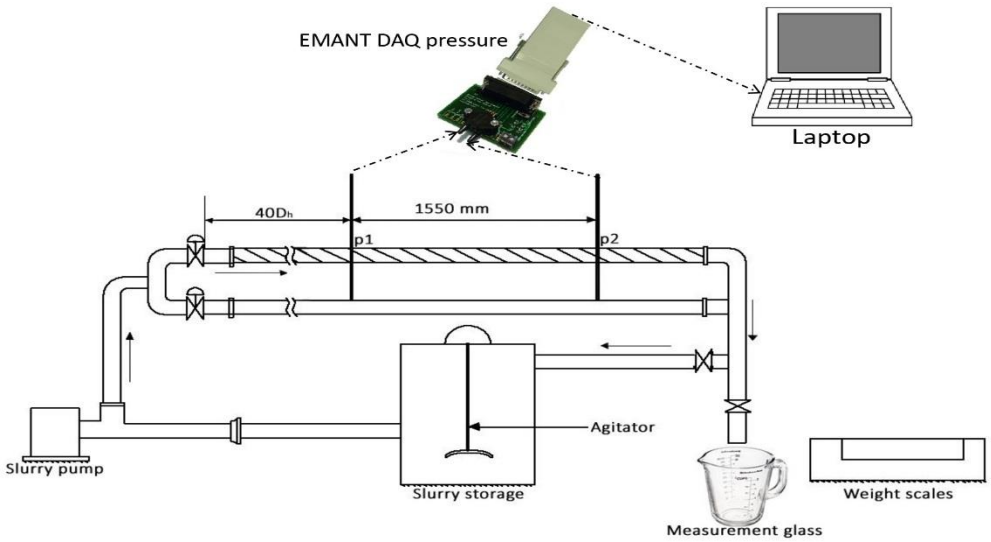


**Figure 2** Schematic diagram of the test pipe

The test ash particles used were obtained from the mud eruption on Semau Island, Indonesia. The slurry obtained was then dried, and the ash particles were measured. As Figure 3 shows, the size range results obtained using scanning electron microscopy (SEM) were 1 μm to 5 μm.

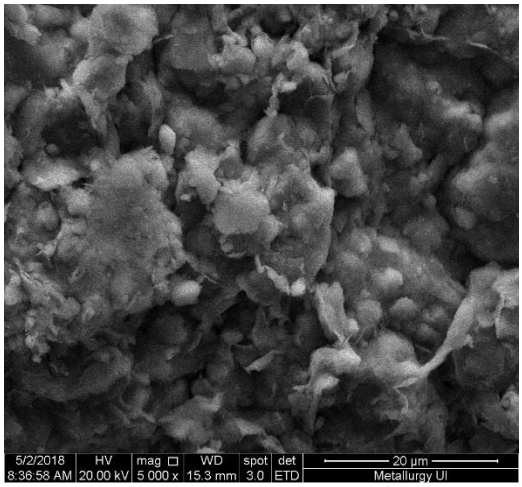


**Figure 3** SEM image of slurry

The slurry from the source eruption was dried and then mixed with pure water in Cw 20%, 30%, and 40%, and the comparison calculation was done using the following equation:

$$C_w = \frac{m_s}{m_w + m_s} x\ 100\% \tag{1}$$

where $m_s$ and $m_w$ are the solid particle mass and pure water mass, respectively. Furthermore, each working fluid regulated in concentration was stirred with an agitator for an hour until it became a homogeneous mixture.

Rheological measurements were carried out at isothermal conditions with a constant temperature of 25°C. The rheological behavior of a non-Newtonian flow such as slurry can be determined by the power law model parameters, such as the power law index ($n$) and the consistency coefficient ($K$). These parameters of $n$ and $K$ can be obtained through scale plots between shear rate, $\gamma = 8\bar{u}/D_h$ and shear stress, $\tau = D_h \Delta P/4L_p$ (Chhabra and Richardson, 1999). The slope and intersection value of the logarithmic graph indicate the values of $n$ and $K$, respectively. It should be noted that testing for the value of $n$ and $K$ uses data from circular pipes. The $n$ value indicates the working fluid as a pseudoplastic fluid and the $K$ values indicate the zero shear of the working fluid. For a complex flow such as a non-Newtonian fluid, the generalized Reynolds number, Re', was used as follows (Kristiawan et al., 2015):

$$\mathrm{Re}' = \frac{\rho_f \bar{u}^{2-n} D_h^n}{K 8^{n-1}} \tag{2}$$

where $\rho_f$ is the density of the working fluid, $\bar{u}$ is the average velocity of the slurry, and $D_h$ is the hydraulic diameter. For friction factor $f$, calculations for non-Newtonian fluids, the Darcy-Weisbach equation was used as follows:

$$f = \frac{D_h}{L} \frac{\Delta P}{(1/2)\rho_f \bar{u}^2} \tag{3}$$

For the maximum drag reduction, the Virk's equation was used as follows:

$$\frac{1}{\sqrt{f}} = 19.0 \log(\mathrm{Re}' \sqrt{f}) - 32.4 \tag{4}$$

The energy loss due to friction can be predicted by using the hydraulic gradient ($I_m$), which is defined as the head loss per unit length (Abulnaga, 2002; Kim et al., 2008). This is an important parameter for evaluating the friction loss, which is defined as the following:

$$I_m = \frac{\Delta p}{\rho_f g L} \tag{5}$$

where Δp is the pressure drop, g is the gravity, and L is the length of the test pipe. To evaluate the additional friction loss due to the solid particles, the solid effect represented by ($I_m$–$I_w$) was used, where $I_w$ is the friction gradient for pure water at the flow rate equal to the slurry flow rate. To calculate the deposition critical velocity $V_{DC}$, the Durand equation was used as follows (Ariyaratne, 2005):

$$V_{DC} = F' \left[2gD_h(\mathrm{s}-1)\right]^{1/2} \tag{6}$$

where $F'$ is an empirical function of the diameter particle and $s$ is relative density.

## 3. Results and Discussion

The first step in determining whether the experimental setup is valid is to conduct a base test. Distilled water was used to ensure the accuracy and reliability of the test apparatus. The value of the initial test by pure water was calculated using a mathematical equation that is well-established to determine the friction factor. For the friction factor, the Hagen-Poiseuille equation for laminar flow (f = 64/Re) and the Blasius equation for turbulent flow ($f = 0.3164Re^{-0.25}$) were used (Kristiawan et al., 2016). For Newtonian fluid, the Reynolds number was used (Re = ρūD/μ). Viscosity was not affected by the shear rate in the Newtonian calculations.

### *3.1. Rheological Characteristics*

The test working fluid gradually flowed through the test pipe under isothermal condition at 25°C. Figure 4 depicts the data of the slurry test with variations of Cw 20%, 30%, and 40%.

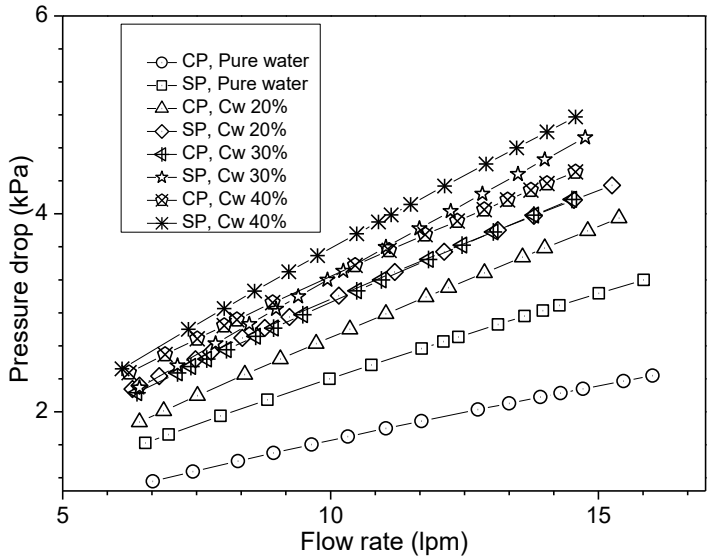


**Figure 4** Comparing pressure drop and flow rate value of data collected

It can be seen that the higher the mixture concentration involved, the greater the pressure drop. The graph shown is similar to that when increasing the pressure drop value when there is an increase in the flow rate variation. The spiral pipe (SP) showed a higher pressure drop than the circular pipe (CP). On the graph, the high mix value of the working fluid of $C_w$ 40% in the spiral pipe showed the highest pressure drop when the flow rate value was gradually increased.

In Figure 5, a comparison of the shear stress and apparent viscosity of the y-axis and the x-axis shear rate is shown. The graph shows an increase in the shear rate value, which results in an increase in shear stress and a decrease in the value of apparent viscosity. This phenomenon indicates that slurry is non-Newtonian fluid classified as pseudoplastic fluid over this range of shear rate. The value of the power law index observed on slurries as working fluids was $n \approx 0.72–0.84$.

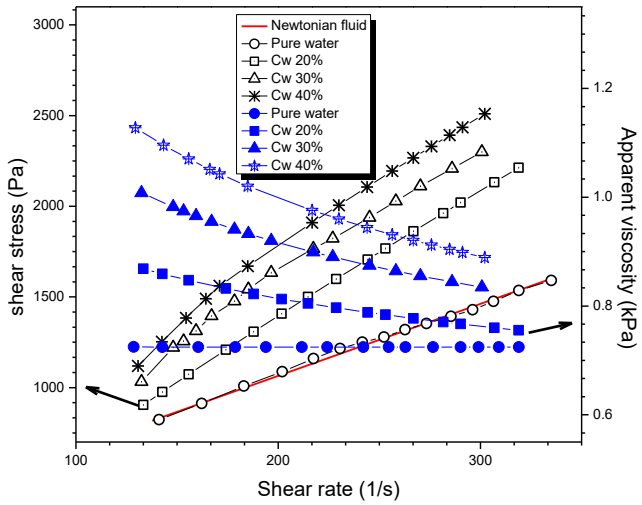


**Figure 5** Representative shear stress and apparent viscosity for slurry flow

It should be noted that data for the circular pipe were used in the calculation of the $n$ and $K$ values. The behavior of pseudoplastic non-Newtonian fluid will result in a decrease in viscosity and an increase in the shear rate value.

### *3.2. Friction Factor*

The calculation results of the friction factor were plotted into a graph, as shown in Figures 6 and 7. In both figures, there are matches between the spiral and circular pipes at the laminar flow has not reduced the drag of friction.

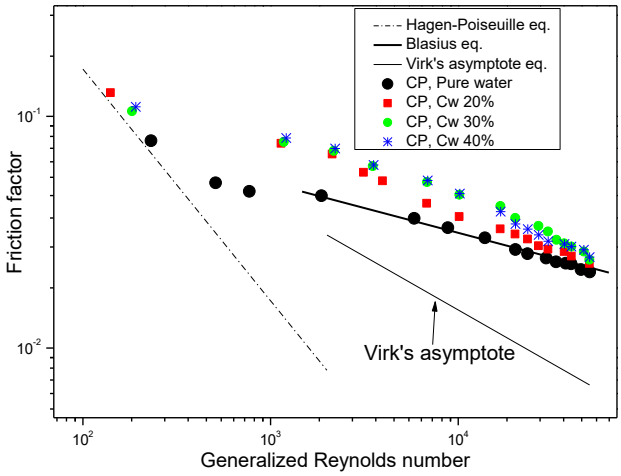


**Figure 6** Friction factor of slurries in a circular pipe

In Figure 6, the Darcy friction factor of the non-Newtonian slurry fits very well with the friction factor of pure water in terms of laminar and turbulent flow. However, they coincide slightly with distilled water and slurry in terms of turbulent flow.

In Figure 7, the trend line of pure water is close to the Hagen-Poiseuille and Blasius equation lines. For the slurry, the more the solid particle concentration was increased, the more the friction value increased. It should be noted that the working fluids phenomenon through the spiral pipe at higher Re' produced lower friction, while the friction decreased in the high turbulent condition. Therefore, spiral pipe geometry can be a trigger to increase the fluctuation of turbulent intensity.

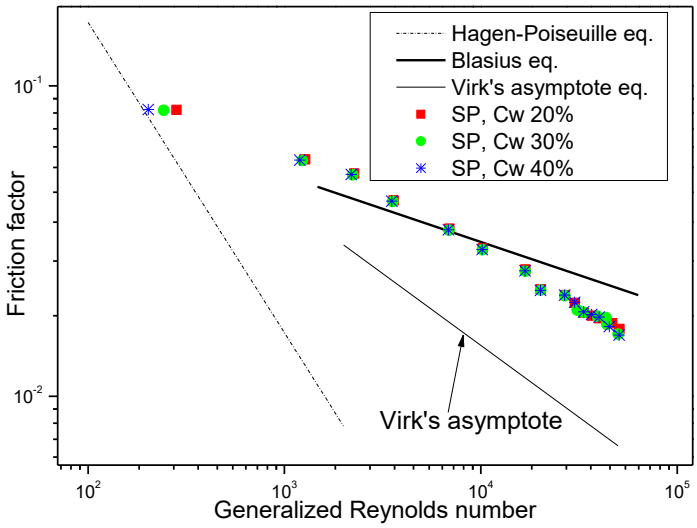


**Figure 7** Friction factor of slurries in spiral pipe

The drag reduction phenomenon in Figure 7 is closely related to the values of $n$ and $K$ because the flow behavior of the pseudoplastic against friction factors is closely related to viscosity. In the graph, drag reduction (DR) gradually increased until the turbulent flow was at maximum value. In the spiral pipe, the higher DR value was 25.8% at Re' $5\times10^4$ and Cw 30%. Further, the trend of the decreasing friction factor below the Blasius equation provides a circumstance that needs to be explored more deeply than what happens in the circular pipe. The spiral pipe geometry also contributes to the prevention of the secondary flow that is likely to occur. This geometry can force fluid to flow at tangential velocity and

thus reduce energy losses due to secondary flow between liquid and particles. It should be noted that the term homogeneous flow is used to express the type of flow that is evenly suspended without precipitation.

### *3.3. Solid Effect*

Figure 8 presents a comparison of hydraulic gradient values with the generalized Reynolds number on a circular pipe and spiral pipe. For circular pipe, it can be seen that at low Re', there is a sharp decrease in the value of the hydraulic gradient, before increasing at Re' $3\times10^4$. The lowest value of the working fluid was observed at Cw 20%, followed by 30% and the highest at 40%. The critical velocity of each concentration was as follows: Cw 20% was 1.33 m/s, Cw 30% was 1.40 m/s, and Cw 40% was 1.43 m/s. The velocity value immediately after reaching the lowest point value of the hydraulic gradient indicates the velocity value needed as the threshold value for the solid particles to flow. Even though it has the same concentration, the circular pipe needs a higher threshold value to allow the solid particles to flow. The high velocity value required by the circular pipe is due to the need for an energy level large enough to move the particles that settle at the bottom of the pipe.

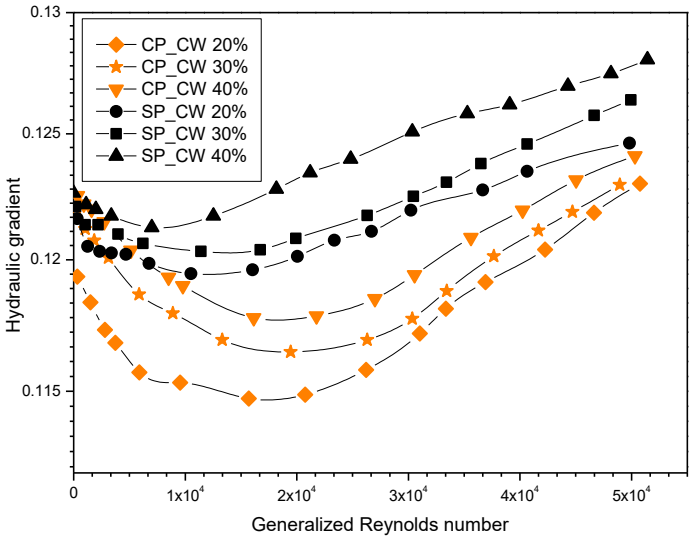


**Figure 8** Comparison of hydraulic gradients and generalized Reynolds numbers

Figure 8 shows a comparison of the hydraulic gradient values of the Reynolds generalized (Re') number in the spiral pipe (SP). It can be seen in the figure that for the low Re' value, the hydraulic gradient value decreases quite sharply and increases when the Re' reaches $1\times10^4$. The increase occurs when the working fluid enters the turbulent zone. The value of the hydraulic gradient that occurs in the spiral pipe for working fluid charged with solid particles is varied at each concentration. The lowest value of the working fluid containing Cw particles is 20%, followed by 30% and the highest at 40%. Through the graph, it can be seen that at the point at which the trend line of the graph increases, the critical velocity of each working fluid is known to have a different value. The critical velocity value for working fluid of Cw 20% is 0.46 m/s, while it is 0.79 m/s for Cw 30% and 1.02 m/s for Cw 40%. The low critical velocity value is influenced by the geometry of the spiral pipe, where the tangential velocity generated becomes a trigger for the particle. In other words, the tangential flow of mud flowing through a spiral pipe specifically affects particles in a process known as vortical motion (Maruyama et al., 1979). The flow pattern allows the

particle to experience a lower threshold of velocity or lower critical velocity in the spiral pipe than in the circular pipe.

The difference between the pressure drop and the inertia force between the pure working fluid and the particle-laden flow in each working fluid flowing in a circular pipe or spiral pipe can predict the effect of solid particles ($I_m$–$I_w$). In Figure 9, the effect of solid particles in a flow with increasing Re' is shown. The average in both circular and spiral pipes at low Re' numbers the solid particle effect is higher and tends to decrease at high Re'. In circular pipe, the effect of solids increases with increasing concentrations of the mixture of particles and decreases with increasing values of the generalized Reynolds number. On the graph, it can be seen that up to Re' $5\times10^4$ there is still a decrease in the particle effects.

The graph also presents the effect of solid volcanic particles on the spiral pipe (SP). The particles have a greater effect when the mixture of solid particle concentrations is higher; this also applies to the spiral pipe and the circular pipe. It can be assumed that the higher the mix of solid particles and water, the greater the interactions of particles in the fluid flow. Although the effect of solid particles causes extra friction loss, an increased velocity value causes the thick working fluid to become thinner. At Re' $3\times10^4$, the particle effect on the spiral pipe starts to be constant while in the circular pipe, the particle effect still tends to decline until the highest Re'. The constant value indicates that, in these conditions, the solid particles have evenly dispersed or are completely homogeneous. Meanwhile, the decreased effects of the solid particles value indicates that the particle dispersion process is still taking place due to the possibility of deposition at the low Re' or agglomeration of solid particles along the pipeline.

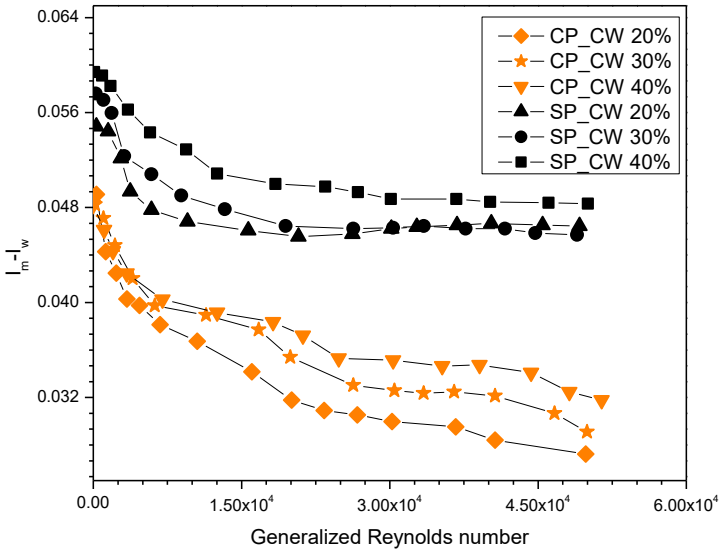


**Figure 9** Comparison of particle effects and generalized Reynolds numbers

## 4. Conclusions

Pressure drop was measured and energy losses calculated to investigate the performance of three-lobed spiral pipe in relation to particle effects. According to the rheological model step, the working fluid considered a pseudoplastic fluid with the *n* values are less than 1 and then by the friction factor calculation for spiral pipe, the higher DR value is 25.8% at Re' $5\times10^4$ and Cw 30%. Spiral pipe geometry can force fluid to flow at a tangential velocity and thus reduce energy losses due to secondary flow between liquid and particles. The fluid velocity value immediately after reaching the lowest point value of the hydraulic gradient indicates the velocity value needed as the threshold value in order for

the solid particles to flow. The lowest value reaches limit threshold of fluid flow on this experiment is value on the spiral pipe. The critical velocity of each concentration in the circular pipe is 1.33 m/s for Cw 20%, 1.40 m/s for Cw 30%, and 1.43 m/s for Cw 40%. Meanwhile, the critical velocity value for working fluid in the spiral pipe is 0.46 m/s for Cw 20%, 0.79 m/s for Cw 30%, and 1.02 m/s for Cw 40%. The low critical velocity value is influenced by the geometry of the spiral pipe, where the tangential velocity generated becomes a trigger for the particle.

## Acknowledgements

This research was funded by a Penelitian Dasar Grant of the Research, Technology and Higher Education Ministry, Indonesia, 2020. NKB-1792/UN2.R3.1/HKP.05.00/2019

## References

Abulnaga, B.E., 2002. *Slurry Systems Handbook*. New York: *McGraw-Hill*

Ariyaratne, C., 2005. *Design and Optimisation of Swirl Pipes and Transition Geometries for Slurry Transport.* Dissertation, Doctoral Program, University of Nottingham, United Kingdom

Chhabra, R.P., Richardson, J.F., 1999. *Non-Newtonian Flow in the Process Industries: Fundamentals and Engineering Applications.* 1st Edition. Butterworth-Heinemann, Oxford, UK

Deka, B., Sharma, R., Mandal, A., Mahto, V., 2018. Synthesis and Evaluation of Oleic Acid Based Polymeric Additive as Pour Point Depressant to Improve Flow Properties of Indian Waxy Crude Oil. *Journal of Petroleum Science and Engineering,* Volume 170, pp. 105–111

Gad-el-Hak, M., Pollard, A., Bonnet, J-P., 2003. *Flow Control: Fundamentals and Practices.* Germany: Springer Science & Business Media

Ganeshalingam, J., 2002. *Swirl-Induction for Improved Solid-Liquid Flow in Pipes.* University of Nottingham

Kim, C., Lee, M., Han, C., 2008. Hydraulic Transport of Sand-water Mixtures in Pipelines Part I. Experiment. *Journal of Mechanical Science and Technology*, Volume 22(12), pp. 2534–2541

Kristiawan, B., Kamal, S., Suhanan., Yanuar., 2015. A Modified Power Law Approach for Rheological Titania Nanofluids Flow Behavior in a Circular Conduit. *Journal of Nanofluids*, Volume 4(2), pp. 187–195

Kristiawan, B., Kamal, S., Yanuar., 2016. Thermo-Hydraulic Characteristics of Anatase Titania Nanofluids Flowing through a Circular Conduit. *Journal of Nanoscience and Nanotechnology*, Volume 16(6), pp. 6078–6085

Mau, S., Yanuar, 2018. Effect of Calcium Carbonate Solution on Drag Reduction in a Pentagon Spiral Pipe. *Akademia Baru*, Volume 1, pp. 41–48

Marbun, J., 2015. Semburan Lumpur Dingin di Semau karena Pergeseran Lempeng Australia *(Cold Mud Eruption in Semau due to Plate Shifting).* Jakarta: Republika

Matousek, V., 2005. Research Developments in Pipeline Transport of Settling Slurries. *Powder Technology*, Volume 156(1), pp. 43–51

Priadi, C.R., Suleeman, E., Darmajanti, L., Novriaty, S., Suwartha, N., Resnawati, R., Handayani, R., Putri, G.L., Felaza, E., Tjahjono, T., 2017. Water Recycling Opportunity in the Business Sectors of Greater Jakarta, Indonesia. *International Journal of Technology*, Volume 8(6), pp. 1031–1039

Selvaraj, P., Sarangan, J., Suresh, S., 2011. Experimental Investigation on Heat Transfer and Friction Factor Characteristics of a Water and Ethylene Glycol Mixture Flow of Internally Grooved Tubes. *International Journal of Chemical Research*, Volume, 3(1), pp. 33–40

Senapati, P., Mishra, B., Parida, A., 2013. Analysis of Friction Mechanism and Homogeneity of Suspended Load for High Concentration Fly Ash & Bottom Ash Mixture Slurry using Rheological and Pipeline Experimental Data. *Powder Technology*, Volume 250, pp. 154–163

Siswantara, A.I., Daryus, A., Darmawan, S., Gunadi, G.G.R., Camalia, R., 2016. CFD Analysis of Slurry Flow in an Anaerobic Digester. *International Journal of Technology*, Volume 7(2), pp. 197–203

Steffe, J.F., 1992. *Rheological Methods in Food Process Engineering*. Second Edition. USA: Freeman Press

Maruyama, T., Kojima, K., Mizushina, T., 1979. The Flow Structure of Slurries in Horizontal Pipes. *Journal of Chemical Engineering of Japan*, Volume 12(3), pp. 177–182

The Jakarta Post, 2015. Drilling, not Quake, Caused Sidoarjo Mud Volcano. Available Online at https://www.thejakartapost.com/news/2015/06/29/drilling-not-quake-caused-sidoarjo-mud-volcano-paper.html

Watanabe, K., Maeda, T., Iwata, T., Kato, H., 1984. Flow in a Spiral Tube: 1st Report, Velocity Distribution and Pressure Drop. *Bulletin of JSME*, Volume 27(228), pp. 1105–1111

Watanabe, K., Yanuar, 1996. Drag Reduction in Flow through Square and Rectangular Ducts with Highly Water-repellent Walls. *Transactions of the Japan Society of Mechanical Engineers*, Volume 62(601), pp. 1996–1999

Yanuar, Gunawan, Sapjah, D., 2015. Characteristics of Silica Slurry Flow in a Spiral Pipe. *International Journal of Technology*, Volume 6(6), pp. 916–923

Yanuar, Utomo, G.G., Rayhan, F.A., Akbar, M., Pamitran, A.S., 2018. Experimental Investigations of Ice Slurry Flow based on Monoethylene Glycol at High Ice Fractions. *In:* E3S Web of Conferences, EDP Sciences

Yanuar, N., Gunawan, I., Baqi, M., 2012. Characteristics of Drag Reduction by Guar Gum in Spiral Pipes. *Jurnal Teknologi*, Volume 58(2), pp. 95–99